DRFC/CAD EUR-CEA-FC-1576

Propagation and Radiation Characteristics of the Circular Electric, Circular Magnetic and Hybrid Waveguide Modes

J.P. Crenn, C. Charollais

June 1996

PROPAGATION AND RADIATION CHARACTERISTICS OF THE CIRCULAR ELECTRIC, CIRCULAR MAGNETIC AND HYBRID WAVEGUIDE MODES

* J.P. CRENN

* *Association EURATOM-CEA sur la Fusion*
Département de Recherches sur la Fusion Contrôlée
Centre d'Études de Cadarache
13108 St Paul-lez-Durance (FRANCE)

** C. CHAROLLAIS

** *INSA de Rouen, Place Emile Blondel*
B.P. 8 - 76131 Mont Saint Aignan Cedex (FRANCE)

SOMMAIRE

ABSTRACT

The field distributions and propagation constants of the circular electric, circular magnetic and hybrid modes of oversized waveguides are expressed, taking the effects of walls into account. These effects are described by wall functions which depend on surface impedances of the wall, and are determined for different types of guides. The near and far field patterns are derived in the case of real wall functions. It is shown that, for very oversized waveguides, the terms containing wall functions can be ignored in the calculations, and it results that the expressions of fields and propagation constants become independent of the types of waveguides. An application to corrugated waveguides for Electron Cyclotron Resonance Heating experiments shows the variations of the radiation characteristics versus geometric parameters of the corrugations and determines the ranges of interest for these parameters.

KEY WORDS : Oversized circular waveguides, Dielectric-lined waveguides, Corrugated waveguides, Dielectric rod waveguides, Hybrid modes, Radiation patterns.

I. INTRODUCTION

Oversized waveguides carrying the fundamental hybrid mode HE_{11} are widely used in infrared and millimeter waves devices because of the excellent propagation and radiation properties of this mode : low attenuation in oversized waveguides, linear polarization, azimuthal symmetry and Gaussian beam-like radiation pattern.

Moreover, in these types of overmoded waveguides, other hybrid modes, and circular electric or circular magnetic modes, can propagate, but are normally considered as spurious modes in experiments.

For all these modes, the propagation and radiation behaviors depend mainly on the wavelength and guide diameter, and, although usually neglected, on the surface impedances of the wall. Taking into account the wall characteristics of the guide, this paper deals with general expressions of the field inside the guide and in the radiation patterns. Five basic types of oversized circular waveguides, supporting circular electric, circular magnetic or hybrid modes, are considered [1] [2] : hollow dielectric or weakly conducting waveguides [3] [4], dielectric-lined waveguides [5] [6], metallic corrugated waveguides [7] [8] [9], and dielectric rod waveguides [1] [6] (Fig. 1).

The paper begins in Section II with the field expressions of the modes inside the guide.

These expressions contain four wall functions : X , Y , Δ and Σ which depend on the surface impedances of the wall. The effects of these wall functions on the field configurations and propagation constants of the modes are discussed. In Section III, the wall functions are calculated for each of the five basic types of waveguides mentioned above.

General relations, giving the near and far field patterns in the cases of real wall functions, are derived in Section IV. More simple relations for the far field region are also investigated. The effects of the wall functions on the radiation characteristics are considered. The section V deals with the mode power and cross-polarization power in relation with the amplitude of the radiated fields.

An application to corrugated waveguides is made in Section VI, in order to determine the variations of the radiated field patterns as a function of the geometric parameters of the corrugations. Waveguides used in transmission lines for Electron Cyclotron Resonance Heating (ECRH) experiments at 110 and 118 GHz on the Tore Supra Tokamak, are considered in this application [10] [11].

II. WAVEGUIDE MODES

Many fundamental works have been made about the field configurations and the propagations of modes in the five types of waveguides that we consider. By using the results obtained by Marcatili and Schmeltzer [3] Degnan [4] Dragone [1] [6] [7] Clarricoats and Olver [9] and Crenn [2], we derive a set of general relations for the modes, which include four wall functions X, Y, Δ and Σ. These functions have different expressions, depending on the surface impedances of each type of guide. According to an usual notation [4] the modes are designated TE_{om} for the circular electric modes, TM_{om} for the circular magnetic modes, EH_{nm} and HE_{nm} for the hybrid modes, where n and m are positive integers. The fundamental mode is designated HE_{11} in this notation.

Let us consider a circular waveguide of radius a, and the coordinate systems defined in Fig. 2. The components of the Electric fields of modes inside the guide are written as :

$$\left.\begin{matrix} E_x \\ E_y \\ E_z \end{matrix}\right\} \exp j(\omega t - \gamma z)$$

where E_x, E_y, E_z are the amplitudes of the components, ω the angular frequency, and γ the propagation constant of the mode. Similarly, the amplitudes of the magnetic field components are noted H_x, H_y and H_z. The amplitudes of the components for the various types of modes inside the guide, are derived as :

- **TM_{om} ($m \geq 1$)**

$$\begin{aligned} E_x &= EJ_1\left(K_{my}\frac{\rho}{a}\right)\cos\phi \\ E_y &= EJ_1\left(K_{my}\frac{\rho}{a}\right)\sin\phi \\ E_z &= jE\,\frac{u_{1m}}{ka}J_0\left(K_{my}\frac{\rho}{a}\right) \qquad (1) \\ H_x &= -\frac{E_y}{Z_0} \\ H_y &= \frac{E_x}{Z_0} \\ H_z &= 0\,. \end{aligned}$$

- **TE_{om} ($m \geq 1$)**

$$E_x = -EJ_1\left(K_{mx}\frac{\rho}{a}\right)\sin\phi$$

$$E_y = EJ_1\left(K_{mx}\frac{\rho}{a}\right)\cos\phi$$

$$E_z = 0 \qquad (2)$$

$$H_x = -\frac{E_y}{Z_0}$$

$$H_y = \frac{E_x}{Z_0}$$

$$H_z = -j\,\frac{E}{Z_0}\,\frac{u_{1m}}{ka}\,J_0\left(K_{mx}\frac{\rho}{a}\right)$$

- **HE_{nm} ($n, m \geq 1$)**

$$E_x = E\left[J_{n-1}\left(K_{n-1,\,m}\frac{\rho}{a}\right)\cos\left[(n-1)\phi+\theta\right]\right.$$

$$\left.+\frac{\Delta u^2_{n-1,\,m}}{4\,n\,ka}J_{n+1}\left(K_{n-1,\,m}\frac{\rho}{a}\right)\cos\left[(n+1)\phi+\theta\right]\right]$$

$$E_y = E\left[-J_{n-1}\left(K_{n-1,\,m}\frac{\rho}{a}\right)\sin\left[(n-1)\phi+\theta\right]\right.$$

$$\left.+\frac{\Delta u^2_{n-1,\,m}}{4\,n\,ka}J_{n+1}\left(K_{n-1,\,m}\frac{\rho}{a}\right)\sin\left[(n+1)\phi+\theta\right]\right]$$

$$E_z = -jE\frac{u_{n-1,\,m}}{ka}J_n\left(K_{n-1,\,m}\frac{\rho}{a}\right)\cos\left(n\phi+\theta\right) \qquad (3)$$

$$H_x = -\frac{E_y}{Z_0}$$

$$H_y = \frac{E_x}{Z_0}$$

$$H_z = -\frac{E_z}{Z_0}\tan\left(n\phi+\theta\right)$$

- **EH_{nm} ($n, m \geq 1$)**

$$E_x = E\left[J_{n+1}\left(K_{n+1,m}\frac{\rho}{a}\right)\cos\left[(n+1)\phi+\theta\right] - \frac{\Delta u_{n+1,m}^2}{4\,n\,ka}J_{n-1}\left(K_{n+1,m}\frac{\rho}{a}\right)\cos\left[(n-1)\phi+\theta\right]\right]$$

$$E_y = E\left[J_{n+1}\left(K_{n+1,m}\frac{\rho}{a}\right)\sin\left[(n+1)\phi+\theta\right] + \frac{\Delta u_{n+1,m}^2}{4\,n\,ka}J_{n-1}\left(K_{n+1,m}\frac{\rho}{a}\right)\sin\left[(n-1)\phi+\theta\right]\right]$$

$$E_z = jE\frac{u_{n+1,m}}{ka}J_n\left(K_{n+1,m}\frac{\rho}{a}\right)\cos(n\phi+\theta) \qquad (4)$$

$$H_x = -\frac{E_y}{Z_0}$$

$$H_y = \frac{E_x}{Z_0}$$

$$H_z = -\frac{E_z}{Z_0}\tan(n\phi+\theta).$$

and the complex propagation constants γ of the modes are obtained as :

- **TM_{om}**

$$\gamma = k\left[1 - \frac{1}{2}\left(\frac{u_{1m}}{ka}\right)^2\left(1-\frac{2Y}{ka}\right)\right] \qquad (5)$$

- **TE_{om}**

$$\gamma = k\left[1 - \frac{1}{2}\left(\frac{u_{1m}}{ka}\right)^2\left(1-\frac{2X}{ka}\right)\right] \qquad (6)$$

- **HE_{nm}**

$$\gamma = k\left[1 - \frac{1}{2}\left(\frac{u_{n-1,m}}{ka}\right)^2\left(1-\frac{\Sigma}{ka}\right)\right] \qquad (7)$$

- **EH_{nm}**

$$\gamma = k\left[1 - \frac{1}{2}\left(\frac{u_{n+1,\,m}}{ka}\right)^2\left(1 - \frac{\Sigma}{ka}\right)\right] \tag{8}$$

where E is a constant field amplitude, θ is a constant azimuthal angle, $k = 2\pi/\lambda$ is the free space propagation constant, λ is the free space wavelength, u_{nm} is the m th root of the Bessel function $J_n(x)$ and Z_0 is the impedance of free space. This impedance is related to the free space dielectric constant ε_0 and the free space magnetic permeability μ_0 by $Z_0 = \sqrt{\frac{\mu_0}{\varepsilon_0}}$. The parameters K_{mx} , K_{my} and K_{nm} are defined as :

$$K_{mx} = u_{1m}\left(1 - \frac{X}{ka}\right) \tag{9}$$

$$K_{my} = u_{1m}\left(1 - \frac{Y}{ka}\right) \tag{10}$$

$$K_{nm} = u_{nm}\left(1 - \frac{\Sigma}{2ka}\right) \tag{11}$$

The functions X , Y , Δ and Σ are defined and expressed in Section III for each of the five types of waveguides under examination.

The following inequalities have been assumed in the calculations of Eqs (1) to (11), [1] [3] [7] :

$$\begin{cases} ka >> 1 \\ ka >> |X| \\ ka >> |Y| \\ k >> |\gamma - k| \end{cases} \tag{12}$$

These inequalities restric the analysis to very oversized waveguides and low order modes for which the propagation constant γ is nearly equal to that of free space. Moreover, by using the inequalities (12), the terms with power of λ/a larger than one have been neglected in the derivation of the field components. Terms with high power of λ/a have also been omitted in the expressions of γ.

Let the propagation constant γ be written as :

$$\gamma = \beta - j\alpha \tag{13}$$

where β is the phase constant and α the attenuation constant of each mode.

By limiting the calculations to the lower order terms for λ/a , the expressions of α and β are derived as :

- **TM_{om}**

$$\beta = k\left[1 - \frac{1}{2}\left(\frac{u_{1m}}{ka}\right)^2\right] \tag{14}$$

$$\alpha = -\frac{1}{a}\left(\frac{u_{1m}}{ka}\right)^2 \mathrm{Im}(Y) \tag{15}$$

- **TE_{om}**

$$\beta = k\left[1 - \frac{1}{2}\left(\frac{u_{1m}}{ka}\right)^2\right] \tag{16}$$

$$\alpha = -\frac{1}{a}\left(\frac{u_{1m}}{ka}\right)^2 \mathrm{Im}(X) \tag{17}$$

- **HE_{nm}**

$$\beta = k\left[1 - \frac{1}{2}\left(\frac{u_{n-1,\,m}}{ka}\right)^2\right] \tag{18}$$

$$\alpha = -\frac{1}{2a}\left(\frac{u_{n-1,\,m}}{ka}\right)^2 \mathrm{Im}(\Sigma) \tag{19}$$

- **EH_{nm}**

$$\beta = k\left[1 - \frac{1}{2}\left(\frac{u_{n+1,\,m}}{ka}\right)^2\right] \tag{20}$$

$$\alpha = -\frac{1}{2a}\left(\frac{u_{n+1,\,m}}{ka}\right)^2 \mathrm{Im}(\Sigma) \tag{21}$$

where Im means Imaginary part.

It is of interest to analyze the effects of the wall functions X , Y , Δ and Σ , on the field configurations and propagation constants of the modes. First, in many situations, the values of λ/a are very small, and it can be assumed that the functions $\frac{|X|}{ka}$, $\frac{|Y|}{ka}$,

$\frac{|\Delta|}{ka}$ and $\frac{|\Sigma|}{ka}$ are null. All the relations giving the field distributions and propagation constants of the modes become independent of the wall characteristics and the same, for all types of guides. The attenuation becomes null in this assumption. Then, if we consider the HE_{1m} modes and put $\theta = 0$ in Eq (3), the main polarization of the field corresponds to E_x, and the cross-polarized field to E_y. If $\frac{|\Delta|}{ka}$ is neglected, the cross-polarized field becomes null for these modes. Moreover, it can be shown, that if the terms containing the functions X, Y, Δ and Σ are neglected, the transverse field E_t, defined by $E_t = \sqrt{E_x^2 + E_y^2}$, has an azimuthal symmetry for each mode. This is no more true for the hybrid modes, when the wall functions are taken into account.

III. WALL FUNCTIONS

III.1.Definitions

The field components and propagation constants of the modes contain the functions X, Y, Δ and Σ which depend on the surface impedances of the wall.

The X and Y functions are defined as :

$$X = -j\frac{E_\phi}{H_z}\cdot\frac{1}{Z_0} \qquad (22)$$

$$= -j\frac{Z_\phi}{Z_0}$$

$$Y = j\frac{H_\phi}{E_z}Z_0 \qquad (23)$$

$$= -j\frac{Z_0}{Z_z}$$

where E_ϕ, E_z and H_ϕ, H_z are electric and magnetic field components in the cylindrical coordinate system (Fig. 2), Z_ϕ is the transverse surface impedance and Z_z is the longitudinal surface impedance of the wall.

For the Δ and Σ functions, it comes :

$$\Delta = Y - X \tag{24}$$

$$= j\left(\frac{Z_\phi}{Z_0} - \frac{Z_0}{Z_z}\right)$$

$$\Sigma = Y + X \tag{25}$$

$$= -j\left(\frac{Z_\phi}{Z_0} + \frac{Z_0}{Z_z}\right)$$

By using results obtained by Dragone [1] and Crenn [2], the functions X and Y are expressed below for the five basic types of waveguides. Then, the other functions : Δ and Σ, can be derived easily from Eqs (24) and (25).

III.2.Hollow dielectric waveguides

The functions X and Y are given by :

$$X = \frac{-j}{\sqrt{\nu^2 - 1}} \tag{26}$$

$$Y = \frac{-j\,\nu^2}{\sqrt{\nu^2 - 1}} \tag{27}$$

where ν is the refractive index of the wall material.

III.3.Conducting waveguides

The calculation yields :

$$X = \frac{\sin \varphi_1 - j \cos \varphi_1}{\nu_1} \tag{28}$$

$$Y = \frac{1-\nu_1^2}{\nu_1} \sin \varphi_1 - j\frac{1+\nu_1^2}{\nu_1} \cos \varphi_1 \tag{29}$$

where the parameters ν_1 and φ_1 are related to the complex refractive index $\bar{\nu}$ by :

$$\bar{\nu}_1 = \nu_1 \exp(j\varphi_1) = \sqrt{\bar{\nu}^2 - 1} \tag{30}$$

and are expressed as :

$$\nu_1 = \left[(\varepsilon_r - 1)^2 + \frac{\sigma^2}{\varepsilon_0^2 \omega^2} \right]^{1/4} \tag{31}$$

$$\varphi_1 = \frac{1}{2} \text{ Arc tan } \frac{\sigma}{\varepsilon_0 \omega (1 - \varepsilon_r)} \tag{32}$$

where σ is the conductivity of the wall, ε_0 the free space dielectric constant, and ε_r the relative dielectric constant of the wall.

It must be emphasized that, for large values of the conductivity σ, the inequalities (12) are no more valid and this type of guide cannot support the hybrid modes. This is true for smooth metallic waveguides at microwave frequencies.

III.4.Dielectric-lined waveguides

The functions X and Y are derived as :

$$X = \frac{\tan \vartheta}{\sqrt{\nu^2 - 1}} - j \frac{R_s}{Z_0} \left(1 + \tan^2 \vartheta \right) \tag{33}$$

$$Y = \frac{-\nu^2}{\sqrt{\nu^2 - 1} \tan \vartheta} - j \frac{R_s}{Z_0} \frac{\nu^4}{\nu^2 - 1} \frac{1 + \tan^2 \vartheta}{\tan^2 \vartheta} \tag{34}$$

where :

$$\vartheta = kd \sqrt{\nu^2 - 1} \tag{35}$$

and, R_s is the surface resistivity of the metallic wall, defined as :

$$R_s = \sqrt{\frac{\omega \mu_0}{2 \sigma}} \tag{36}$$

μ_0 is the free space magnetic permeability.

The other parameters are defined in Fig. 3.

III.5.Corrugated waveguides

The functions X and Y are obtained as :

$$X = -j\frac{R_s}{Z_0} \tag{37}$$

$$Y = -\frac{Z_0 X_p}{R_s^2 + X_p^2} - j\frac{Z_0 R_s}{R_s^2 + X_p^2} \tag{38}$$

where jX_p is a reactance, defined by :

$$X_p = Z_0 \frac{w}{h}\frac{\tan kd}{1+\frac{2\tan kd}{ka}} \tag{39}$$

the parameters w , h and d are defined in Fig. 4.

It must be noted that the effect of finite waveguide diameter has been included in Eq (39), according to the expression of the longitudinal reactance by Doane [8] and Clarricoats and Saha [12].

III.6.Dielectric rod waveguides

The functions X and Y are given by :

$$X = \frac{\nu}{\sqrt{\nu^2 - 1}} \tag{40}$$

$$Y = \frac{1}{\nu\sqrt{\nu^2 - 1}} \tag{41}$$

IV. RADIATION PATTERNS

Calculations of the near and far field patterns of some hybrid modes have been made by Degnan [4] taking into account the Fresnel approximations to scalar diffraction theory, and ignoring the terms which include wall characteristics. From the expressions of the modes given by Eqs (1) to (4) which contain the wall functions, the fields in the near and far field regions are derived using results obtained by Degnan. The calculations are

made only in the simple case where the wall functions X , Y , Δ and Σ are real, which means there are no power losses in the guide. Consequently, it is assumed that $R_s = 0$. Only three types of waveguides, having no power losses can be considered : dielectric-lined waveguide, corrugated waveguide and dielectric rod waveguide. Their wall functions are obtained as follows :

Dielectric-lined waveguides

$$X = \frac{\tan \vartheta}{\sqrt{\nu^2 - 1}} \tag{42}$$

$$Y = \frac{-\nu^2}{\sqrt{\nu^2 - 1}\ \tan \vartheta} \tag{43}$$

$$\Delta = \frac{-1}{\sqrt{\nu^2 - 1}} \left(\tan \vartheta + \frac{\nu^2}{\tan \vartheta} \right) \tag{44}$$

$$\Sigma = \frac{1}{\sqrt{\nu^2 - 1}} \left(\tan \vartheta - \frac{\nu^2}{\tan \vartheta} \right) \tag{45}$$

Corrugated waveguides

$$X = 0 \tag{46}$$

$$Y = \Delta = \Sigma = -\frac{Z_0}{X_p} \tag{47}$$

where X_p is given by Eq (39).

Dielectric rod waveguides

The functions X and Y are given by Eqs (40) and (41). For Δ and Σ , it comes :

$$\Delta = -\frac{\sqrt{\nu^2 - 1}}{\nu} \tag{48}$$

$$\Sigma = \frac{\nu^2 + 1}{\nu\sqrt{\nu^2 - 1}} \tag{49}$$

Moreover the ratio λ/a is assumed to be small, so that, according to Eqs (1) to (4), the field components E_z and H_z are small with regard to the transverse components. Consequently, we restrict the analysis to the transverse fields of the radiated modes.

Another reason for ignoring the z-components of the field is that measuring horns used in radiation pattern experiments, are generally weakly coupled to this axial field component.

The electric field amplitudes of the radiated modes are derived in the near and far field regions as :

- **TM_{om} ($m \geq 1$)**

$$E_x = A\frac{ka^2}{z}\cos\phi\sqrt{M_{my}^2 + N_{my}^2} \qquad (50)$$

$$E_y = A\frac{ka^2}{z}\sin\phi\sqrt{M_{my}^2 + N_{my}^2}$$

- **TE_{om} ($m \geq 1$)**

$$E_x = -A\frac{ka^2}{z}\sin\phi\sqrt{M_{mx}^2 + N_{mx}^2} \qquad (51)$$

$$E_y = A\frac{ka^2}{z}\cos\phi\sqrt{M_{mx}^2 + N_{mx}^2}$$

- **HE_{nm} ($n, m \geq 1$)**

$$E_x = A\frac{ka^2}{z}\left[\sqrt{M_{n-1,m}^2 + N_{n-1,m}^2}\cos\left[(n-1)\phi + \theta\right]\right.$$
$$\left. + \frac{\Delta u_{n-1,m}^2}{4\,n\,ka}\sqrt{M_{nm}'^2 + N_{nm}'^2}\cos\left[(n+1)\phi + \theta\right]\right] \qquad (52)$$

$$E_y = -A\frac{ka^2}{z}\left[\sqrt{M_{n-1,m}^2 + N_{n-1,m}^2}\sin\left[(n-1)\phi + \theta\right]\right.$$
$$\left. - \frac{\Delta u_{n-1,m}^2}{4\,n\,ka}\sqrt{M_{nm}'^2 + N_{nm}'^2}\sin\left[(n+1)\phi + \theta\right]\right]$$

- **EH_{nm} (n, m ≥ 1)**

$$E_x = A\frac{ka^2}{z}\left[\sqrt{M^2_{n+1,\,m} + N^2_{n+1,\,m}}\,\cos\left[(n+1)\,\phi + \theta\right] - \frac{\Delta u^2_{n+1,\,m}}{4\,n\,ka}\sqrt{M''^2_{n\,m} + N''^2_{n\,m}}\cos\left[(n-1)\,\phi + \theta\right]\right] \tag{53}$$

$$E_y = A\frac{ka^2}{z}\left[\sqrt{M^2_{n+1,\,m} + N^2_{n+1,\,m}}\,\sin\left[(n+1)\,\phi + \theta\right] + \frac{\Delta u^2_{n+1,\,m}}{4\,n\,ka}\sqrt{M''^2_{n\,m} + N''^2_{n\,m}}\,\sin\left[(n-1)\,\phi + \theta\right]\right]$$

where :

$$M_{my} = \int_0^1 \cos\left(\frac{ka^2 s}{2z}\right) J_1\left(K_{my}\sqrt{s}\right) J_1\left(p\sqrt{s}\right) ds \tag{54}$$

$$N_{my} = \int_0^1 \sin\left(\frac{ka^2 s}{2z}\right) J_1\left(K_{my}\sqrt{s}\right) J_1\left(p\sqrt{s}\right) ds \tag{55}$$

$$M_{mx} = \int_0^1 \cos\left(\frac{ka^2 s}{2z}\right) J_1\left(K_{mx}\sqrt{s}\right) J_1\left(p\sqrt{s}\right) ds \tag{56}$$

$$N_{mx} = \int_0^1 \sin\left(\frac{ka^2 s}{2z}\right) J_1\left(K_{mx}\sqrt{s}\right) J_1\left(p\sqrt{s}\right) ds \tag{57}$$

$$M_{nm} = \int_0^1 \cos\left(\frac{ka^2 s}{2z}\right) J_n\left(K_{nm}\sqrt{s}\right) J_n\left(p\sqrt{s}\right) ds \tag{58}$$

$$N_{nm} = \int_0^1 \sin\left(\frac{ka^2 s}{2z}\right) J_n\left(K_{nm}\sqrt{s}\right) J_n\left(p\sqrt{s}\right) ds \tag{59}$$

$$M'_{nm} = \int_0^1 \cos\left(\frac{ka^2 s}{2z}\right) J_{n+1}\left(K_{n-1,\,m}\sqrt{s}\right) J_{n+1}\left(p\sqrt{s}\right) ds \tag{60}$$

$$N'_{nm} = \int_0^1 \sin\left(\frac{ka^2 s}{2z}\right) J_{n+1}\left(K_{n-1,\,m}\sqrt{s}\right) J_{n+1}\left(p\sqrt{s}\right) ds \tag{61}$$

$$M''_{nm} = \int_0^1 \cos\left(\frac{ka^2 s}{2z}\right) J_{n-1}\left(K_{n+1,\,m}\sqrt{s}\right) J_{n-1}\left(p\sqrt{s}\right) ds \qquad (62)$$

$$N''_{nm} = \int_0^1 \sin\left(\frac{ka^2 s}{2z}\right) J_{n-1}\left(K_{n+1,\,m}\sqrt{s}\right) J_{n-1}\left(p\sqrt{s}\right) ds \qquad (63)$$

where :

$s = \left(\frac{\rho_0}{a}\right)^2$, $\rho = \rho_0$ in the guide aperture (i.e. for $z = 0$), $p = ka\frac{\rho}{z}$, and A is a constant amplitude.

Like in Section II, the inequalities (12) have been assumed in the calculations, and the terms with power of λ/a larger than one have been neglected.

If we consider now the far field region, the values of z become large so that :

$$\cos\left(\frac{ka^2 s}{2z}\right) \approx 1 \qquad (64)$$

$$\sin\left(\frac{ka^2 s}{2z}\right) \approx 0$$

The terms N_{my} , N_{mx} , N_{nm} , N'_{nm} and N''_{nm} become null, while M_{my} , M_{mx} , M_{nm} , M'_{nm} and M''_{nm} are expressed by the following type of integral :

$$I = \int_0^1 J_n(uz)\, J_n(vz)\, z\, dz \qquad (65)$$

This integral I is a Lommel integral which can be solved by either of the relations :

$$I = \frac{1}{u^2 - v^2}\left[u\, J_n(v)\, J_{n+1}(u) - v\, J_n(u)\, J_{n+1}(v)\right] \qquad (66)$$

or :

$$I = \frac{1}{u^2 - v^2}\left[v\, J_{n-1}(v)\, J_n(u) - u\, J_{n-1}(u)\, J_n(v)\right] \qquad (67)$$

Finally, the calculation yields :

$$M_{my} = \frac{2K_{my}}{K_{my}^2 - p^2} J_1(p)\, J_2\left(K_{my}\right) \qquad (68)$$

$$M_{mx} = \frac{2K_{mx}}{K_{mx}^2 - p^2} J_1(p)\, J_2(K_{mx}) \tag{69}$$

$$M_{n-1,\,m} = \frac{2}{K_{n-1,\,m}^2 - p^2}\Big[K_{n-1,\,m}\, J_{n-1}(p)\, J_n(K_{n-1,\,m}) - p\, J_{n-1}(K_{n-1,\,m})\, J_n(p)\Big] \tag{70}$$

$$M_{n+1,\,m} = \frac{2}{K_{n+1,\,m}^2 - p^2}\Big[p\, J_n(p)\, J_{n+1}(K_{n+1,\,m}) - K_{n+1,\,m}\, J_n(K_{n+1,\,m})\, J_{n+1}(p)\Big] \tag{71}$$

$$M'_{n,\,m} = \frac{2}{K_{n-1,\,m}^2 - p^2}\Big[p\, J_n(p)\, J_{n+1}(K_{n-1,\,m}) - K_{n-1,\,m}\, J_n(K_{n-1,\,m})\, J_{n+1}(p)\Big] \tag{72}$$

$$M''_{n,\,m} = \frac{2}{K_{n+1,\,m}^2 - p^2}\Big[K_{n+1,\,m}\, J_{n-1}(p)\, J_n(K_{n+1,\,m}) - p\, J_{n-1}(K_{n+1,\,m})\, J_n(p)\Big] \tag{73}$$

and :

$$N_{my} = N_{mx} = N_{nm} = N'_{nm} = N''_{nm} = 0 \tag{74}$$

By using Eqs (68) to (74) the field relations given by Eqs (50) to (63) may be obtained in the far field region without integral relations.

Other remarks concern the effects of the wall functions on the radiation patterns. For large ka values, the terms containing X, Y, Δ and Σ can be neglected in Eqs (50) to (73).

The field patterns become independent of the type of waveguides, even those with complex wall functions. The same effects as discussed in Section II for the cross-polarization of the HE_{1m} modes and the azimuthal symmetry of the hybrid modes inside the guide, are also true in the radiated field.

V. MODE POWER AND RADIATED FIELDS

The constant azimuthal angle θ is assumed to be null in this Section. As shown in Section II, if we consider the HE_{1m} modes, the main polarization of the field corresponds to E_x and the cross-polarized field to E_y. Let P_x and P_y be the powers corresponding to the field components E_x and E_y. They are given by (Fig. 2) :

$$P_x = \int_{\rho=0}^{\infty}\int_{\phi=0}^{2\pi} \frac{E_x^2}{2Z_0}\,\rho d\rho\, d\phi \tag{75}$$

and :

$$P_y = \int_{\rho=0}^{\infty}\int_{\phi=0}^{2\pi} \frac{E_y^2}{2Z_0}\,\rho d\rho\, d\phi \tag{76}$$

where the abscissa z is made constant in the expressions of E_x and E_y.

By using the field relations in the far field region, given by Eqs (50) to (53) and (68) to (74), the powers P_x and P_y are derived as :

- **TM_{om} ($m \geq 1$)**

$$P_x = A^2 \frac{2\pi a^2}{Z_0}\int_0^{\infty}\left(\frac{K_{my}\,J_2(K_{my})\,J_1(p)}{K_{my}^2 - p^2}\right)^2 pdp \tag{77}$$

$$P_y = P_x \tag{78}$$

- **TE_{om} ($m \geq 1$)**

$$P_x = A^2 \frac{2\pi a^2}{Z_0}\int_0^{\infty}\left(\frac{K_{mx}\,J_2(K_{mx})\,J_1(p)}{K_{mx}^2 - p^2}\right)^2 pdp \tag{79}$$

$$P_y = P_x \tag{80}$$

- **HE_{1m} ($m \geq 1$)**

$$P_x = A^2 \frac{\pi a^2}{2Z_0}\left[\int_0^{\infty} 2M_{om}^2\, pdp + \int_0^{\infty}\left(\frac{\Delta u_{om}^2}{4ka}\right)^2 M_{1m}'^2\, pdp\right] \tag{81}$$

$$P_y = A^2 \frac{\pi a^2}{2Z_0}\int_0^{\infty}\left(\frac{\Delta u_{om}^2}{4ka}\right)^2 M_{1m}'^2\, pdp \tag{82}$$

- **HE_{nm} ($n \geq 2$, $m \geq 1$)**

$$P_x = A^2 \frac{\pi a^2}{2Z_0} \left[\int_0^\infty M_{n-1,\,m}^2 \, pdp + \int_0^\infty \left(\frac{\Delta u_{n-1,\,m}^2}{4\,n\,ka} \right)^2 M_{nm}^{'2} \, pdp \right] \quad (83)$$

$$P_y = P_x \quad (84)$$

- **EH_{1m} ($m \geq 1$)**

$$P_x = A^2 \frac{\pi a^2}{2Z_0} \left[\int_0^\infty M_{2m}^2 \, pdp + \int_0^\infty 2 \left(\frac{\Delta u_{2m}^2}{4\,ka} \right)^2 M_{1m}^{''2} \, pdp \right] \quad (85)$$

$$P_y = A^2 \frac{\pi a^2}{2Z_0} \int_0^\infty M_{2m}^2 \, pdp \quad (86)$$

- **EH_{nm} ($n \geq 2$, $m \geq 1$)**

$$P_x = A^2 \frac{\pi a^2}{2Z_0} \left[\int_0^\infty M_{n+1,\,m}^2 \, pdp + \int_0^\infty \left(\frac{\Delta u_{n+1,\,m}^2}{4\,n\,ka} \right)^2 M_{nm}^{''2} \, pdp \right] \quad (87)$$

$$P_y = P_x \quad (88)$$

It must be noted that in free space, i.e. in a lossless medium, the power expressions given by Eqs (77) to (88) are valid in the near field region as well as in the far field region.

VI. APPLICATION TO CORRUGATED WAVEGUIDES

Corrugated waveguides are currently used in the microwave range, at frequencies lower than 140 GHz at the present time. Indeed, this type of guide is attractive for carrying the fundamental HE_{11} mode with low losses at microwave frequencies [2]. By assuming that $R_s = 0$, the radiated field behaviour of the HE_{11} mode depends only on one wall function Y given by Eq (47). This function Y is related to the radius a of the guide and to the geometric parameters w , h and d of the corrugations by Eqs (39) and (47). The effects of theses parameters on the radiation characteristics of the HE_{11} mode are investigated for a guide of radius $a = 31.75$ mm at the frequency $f = 110$ GHz. This corresponds to typical values of waveguides and frequency for ECRH experiments on

plasma machines. Two parameters are varied in the analysis : h/w and D . The latter is defined by :

$$kd = D.\frac{\pi}{2} \tag{89}$$

This relation shows that $D = 1$ for $kd = \pi/2$ or $d = \lambda/4$ which corresponds to the maximum of X_p :

$$X_p = Z_0 \frac{w}{h} \frac{ka}{2} \tag{90}$$

and to the minimum of the function Y. This value $D = 1$ is of interest, because it corresponds to a minimum effect of the wall on the field distribution, and also to the minimum of the hybrid mode attenuation in the guide when D is varied [2] [8]. On the contrary, the following values of D :

$$D = 0, 2, 4 \ldots 2p \tag{91}$$

involve $X_p = 0$, $|Y| \rightarrow \infty$ and the inequalities (12) are no more valid. The hybrid modes cannot propagate in the guide for values of D close or equal to those in Eq (91). The variations of Y as a function of D are displayed in Fig. 5, where $w/h = 0.5$.

By assuming that $\theta = 0$ in Eq (52), the radiation pattern of E_x, the principal component of the HE_{11} mode is calculated versus the angle α (Fig. 2), for $z = 1.60$ m, which is the beginning of the far field region, and for three values of the angle ϕ : $\phi = 0$, $\pi/4$, $\pi/2$.

The results are shown in Figs 6, 7 and 8. The variations of the 10 dB bandwidth of the central lobes are plotted in Fig. 9 versus D for the three values of ϕ which are considered.

The normalized cross-polarization, that is the ratio $E_y/E_x(0)$ is plotted in Fig. 10 for various values of D , in the case of $\phi = \pi/4$. The cross-polarization power, defined by the ratio $\frac{P_y}{P_y + P_x}$ is also considered. The powers P_x and P_y of the HE_{11} mode are obtained by making $m = 1$ in Eqs (81) and (82). The cross-polarization power of the HE_{11} mode is plotted versus D in Fig. 11.

From all the plots in Figs 5 to 11, it results that the changes in field patterns or cross-polarization may be assumed to be negligible or very small for $0.5 < D < 1.5$, then increase but are kept small for $0.1 < D < 0.5$ and $1.5 < D < 1.9$. The changes become

important and, moreover the validity of the inequalities (12) is not always true, for $0 < D < 0.1$ and $1.9 < D < 2$.

By using Eq (19), the attenuation of the HE_{11} mode is also calculated and is plotted in Fig. 12. There is a good agreement with the field patterns and cross-polarization results : the attenuation is very small in the range $0.5 < D < 1.5$, then increases when $0.1 < D < 0.5$ and $1.5 < D < 1.9$ and finally becomes important for $0 < D < 0.1$ and $1.9 < D < 2$.

The other parameter to be varied in this application, is the ratio w/h . The variations of Y against w/h are plotted in Fig. 13, assuming that the optimal value $D = 1$ is made. The - 10 dB widths of the central lobe of the field patterns have been calculated for the three values of ϕ : $\phi = 0$, $\pi/4$, $\pi/2$ and are plotted against the ratio w/h in Fig. 14. Moreover, the ratio $\frac{P_y}{P_y + P_x}$ of the cross-polarization power to the total power is plotted against the ratio w/h in Fig. 15. As shown by these Figures 13 to 15, the guide works well for $0.1 < w/h < 1$, but not in the range $0 < w/h < 0.1$.

Finally, this application to a waveguide of radius $a = 31.75$ mm carrying the HE_{11} mode at $f = 110$ GHz, shows that the ranges to be considered for the parameters D and w/h are $0.5 < D < 1.5$ and $0.1 < w/h < 1$. These ranges of interest have been determined for a particular value of ka : it is expected that the result would be changed if this parameter ka is varied. It is expected also that the radiation pattern is more sensitive to wall functions for higher order modes than for the HE_{11} mode.

As an example, we consider the transmission line for ECRH experiments on the Tokamak Tore Supra. The working frequencies are $f = 110$ and 118 GHz, and the parameters of the corrugated waveguides are given as :

- **110 GHz waveguides**

d = 0.38 mm

w = 0.66 mm D = 0.557

h = 0.91 mm w/h = 0.726

a = 31.75 mm

- **118 GHz waveguides**

d = 0.64 mm

w = 0.80 mm D = 1.007

h = 1.1 mm w/h = 0.727

a = 31.75 mm

These values of D and w/h are placed in the ranges where the wall functions have only little effects on the field pattern of the HE_{11} mode and usually can be neglected.

VII. CONCLUSION

Wall effects have been taken into account in the calculation of the field configurations and propagation constants of circular electric, circular magnetic and hybrid waveguide modes. These effects are described by wall functions which depend on the surface impedances of the wall and have been determined for five types of circular oversized waveguides. The near and far field patterns have been derived for guides having real wall functions, i.e. without power losses.

It has been shown that the wall functions give spurious effects by creating cross-polarized fields for the HE_{1m} modes and azimuthal asymmetry of the transverse field amplitude for all the hybrid modes. However, the wall effects decrease with increasing values of ka. Consequently, in many experimental situations, these effects can be neglected and the same formulas of mode radiations can be used for all kinds of waveguides.

The case of the corrugated waveguides, which are often used in microwaves, is of special importance. The effects of the geometric parameters of the corrugations on the radiated field patterns of the HE_{11} mode are investigated for a typical case of waveguides for ECRH experiments. The ranges of geometric parameters of the corrugations which have to be used in order to get the best propagation and radiation properties of the HE_{11} mode, have been determined.

Acknowledgement

The authors are grateful to G. Berger By, P. Bibet, P. Garin, M. Pain and J.G. Wegrowe for assistance in the work and review of the manuscript.

REFERENCES

[1] C. Dragone, Bell Syst. Tech. J., 60, 89 (1981).

[2] J.P. Crenn, Int. J. Infrared Millimeter Waves, 14, 1947 (1993).

[3] E.A.J. Marcatili and R.A. Schmeltzer, Bell Syst. Tech. J., 43, 1783 (1964).

[4] J.J. Degnan, Appl. Opt., 12, 1026 (1973).

[5] J.W. Carlin and P. D'Agostino, Bell Syst. Tech. J., 52, 453 (1973).

[6] C. Dragone, I.E.E.E. Trans. Microwave Theory Tech., 28, 704 (1980).

[7] C. Dragone, Bell Syst. Tech. J., 56, 835 (1977).

[8] J. Doane, Infrared and Millimeter Waves, 13, 123, Academic Press (1985)

[9] P.J.B. Clarricoats and A.D. Olver, Corrugated horns for microwave antennas Peter Peregrinus Ltd, London (1984).

[10] M. Pain, G. Berger-By, P. Bibet, G. Bon Mardion, J.J. Capitain, J.P. Crenn, F. Smits, G. Tonon, 17th Symposium on Fusion Technology, Roma, Italy, September 14-18 (1992).

[11] M. Pain, G. Berger-By, G. Bon Mardion, J.M. Bottereau, J.P. Crenn, P. Nouvel, D. Piat, D. Roux, F. Smits, 18th Symposium on Fusion Technology, Karlsruhe, Germany, August 22-26 (1994).

[12] P.J.B. Clarricoats and P.K. Saha, Proc. I.E.E., 118, 1167 (1971).

FIGURE CAPTIONS

Figure 1 : Oversized circular waveguides :

a) Hollow dielectric waveguide

b) Conducting waveguide

c) Dielectric rod waveguide

d) Corrugated waveguide

e) Dielectric-lined waveguide

Figure 2 : Coordinate systems

a) Waveguide and Cartesian coordinates

b) Transverse coordinates

Figure 3 : Dielectric-lined waveguide

Figure 4 : Corrugated waveguide

Figure 5 : Variations of the wall function Y for $w/h = 0.5$

Figure 6 : Radiation patterns of the HE_{11} mode for $\phi = 0$

Figure 7 : Radiation patterns of the HE_{11} mode for $\phi = \pi/4$

Figure 8 : Radiation patterns of the HE_{11} mode for $\phi = \pi/2$

Figure 9 : Variations of the 10 dB bandwidth of E_x referred to the case $D = 1$ and for $w/h = 0.5$

Figure 10 : Cross-polarization of HE_{11} mode normalized to $E_x(0) = 1$ and for $\phi = \pi/4$

Figure 11 : Variations of $\frac{P_y}{P_y + P_x}$ for $w/h = 0.5$

Figure 12 : Attenuation of the HE_{11} mode

Figure 13 : Variations of the wall function Y for $D = 1$

Figure 14 : Variations of the 10 dB bandwidth of E_x referred to the case $w/h = 0.5$ and for $D = 1$

Figure 15 : Variations of $\frac{P_y}{P_y + P_x}$ for $D = 1$

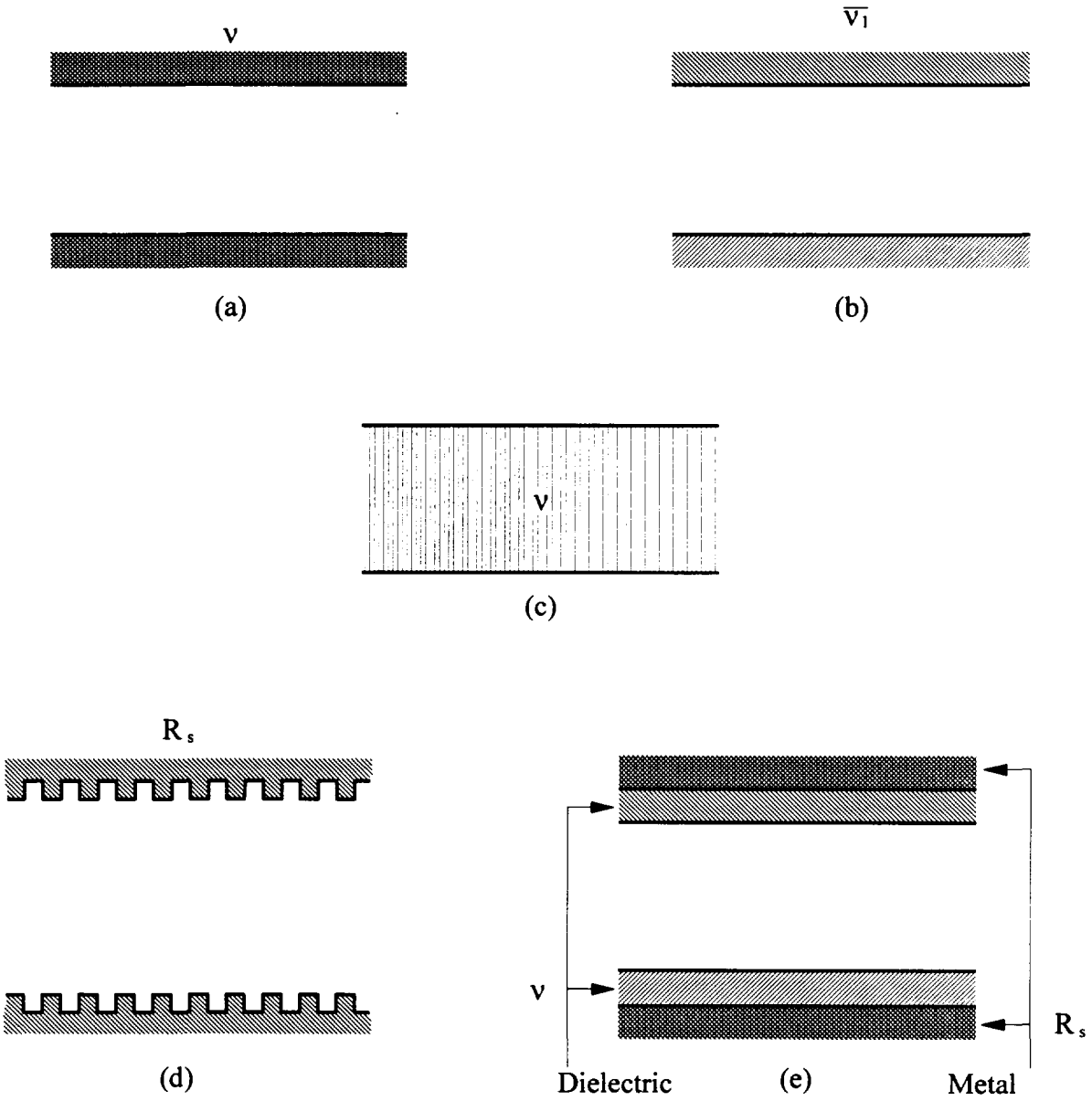

Figure 1 ***: Oversized circular waveguides :***

- ***a) Hollow dielectric waveguide***
- ***b) Conducting waveguide***
- ***c) Dielectric rod waveguide***
- ***d) Corrugated waveguide***
- ***e) Dielectric-lined waveguide***

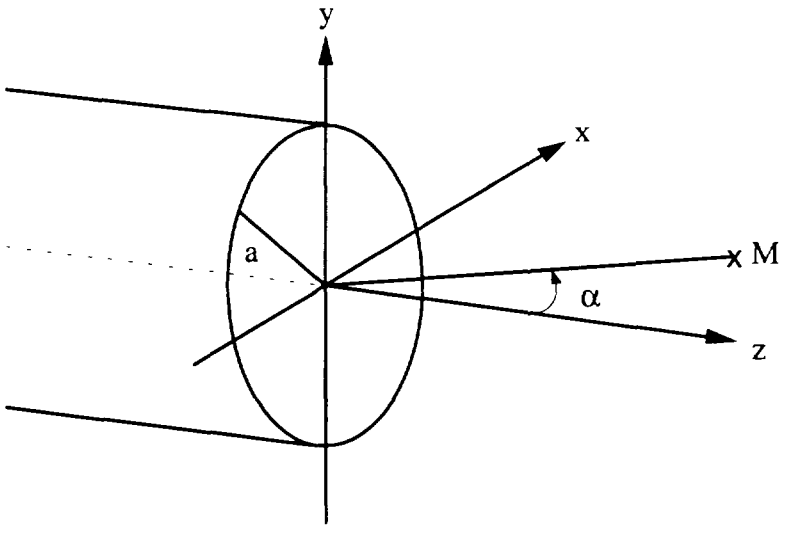

(a)

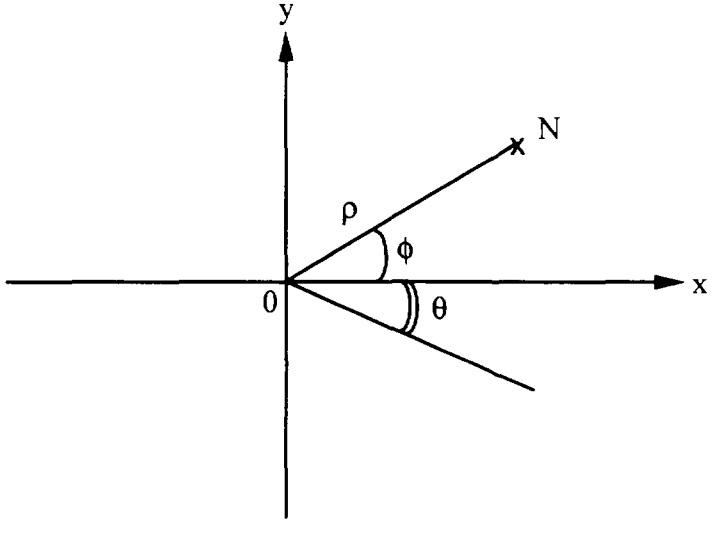

(b)

***Figure 2** : Coordinate systems*

a) Waveguide and Cartesian coordinates

b) Transverse coordinates

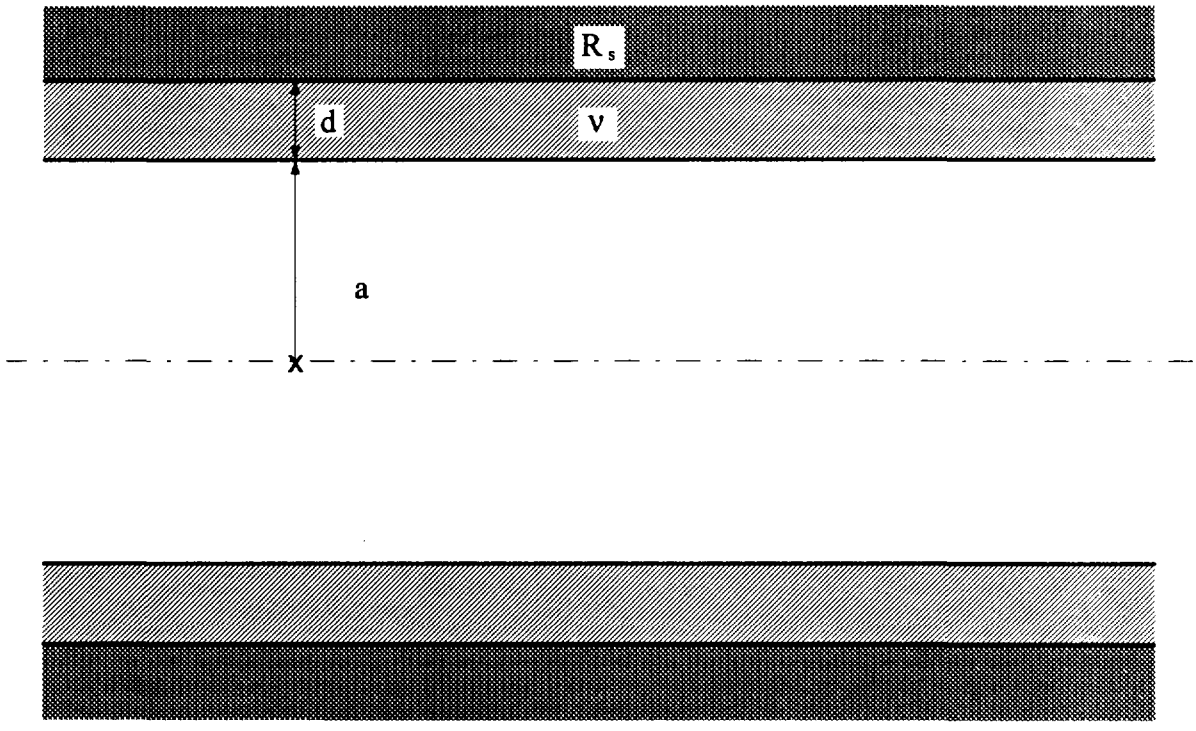

***Figure 3* : Dielectric-lined waveguide**

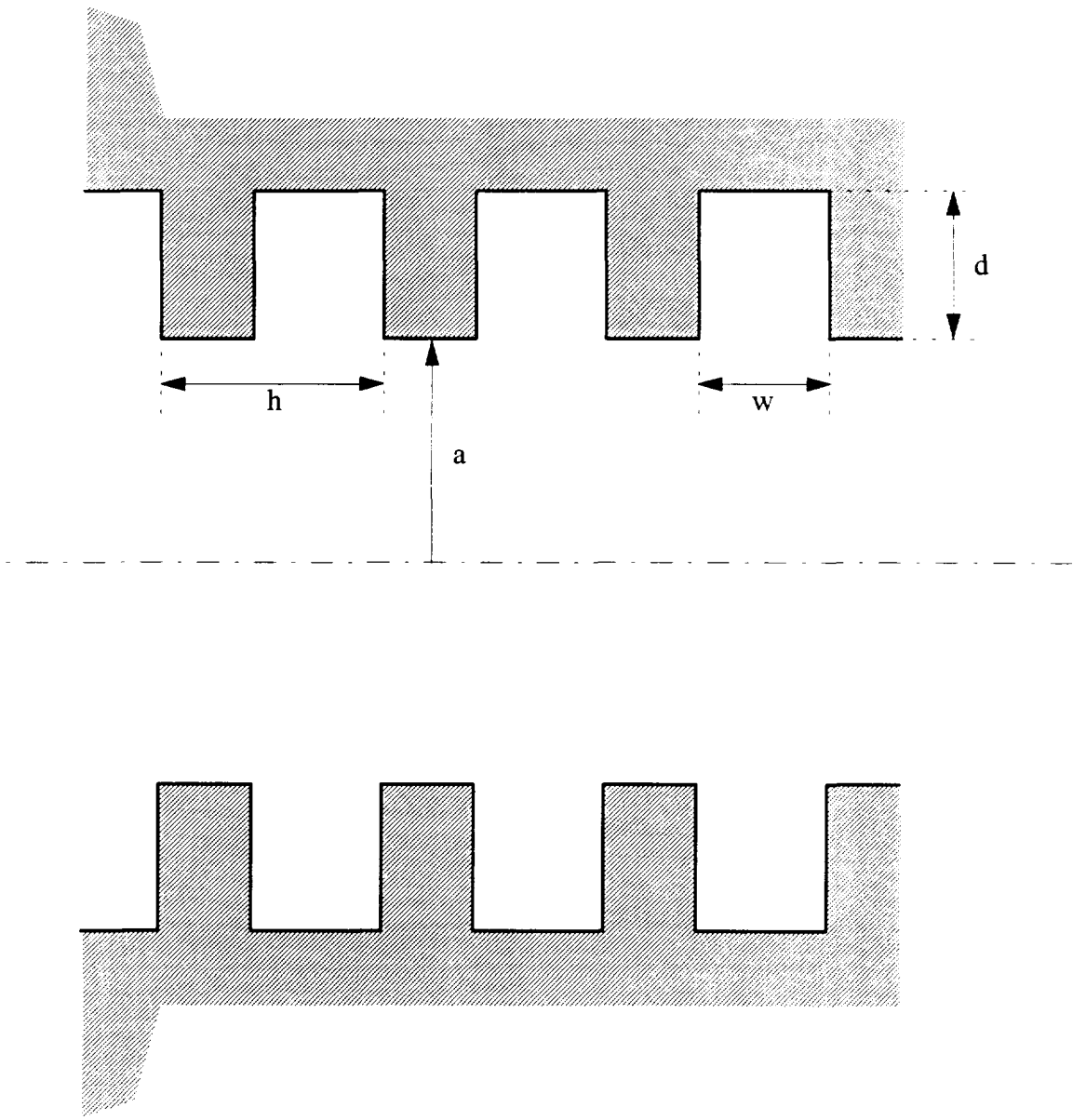

***Figure 4* : Corrugated waveguide**

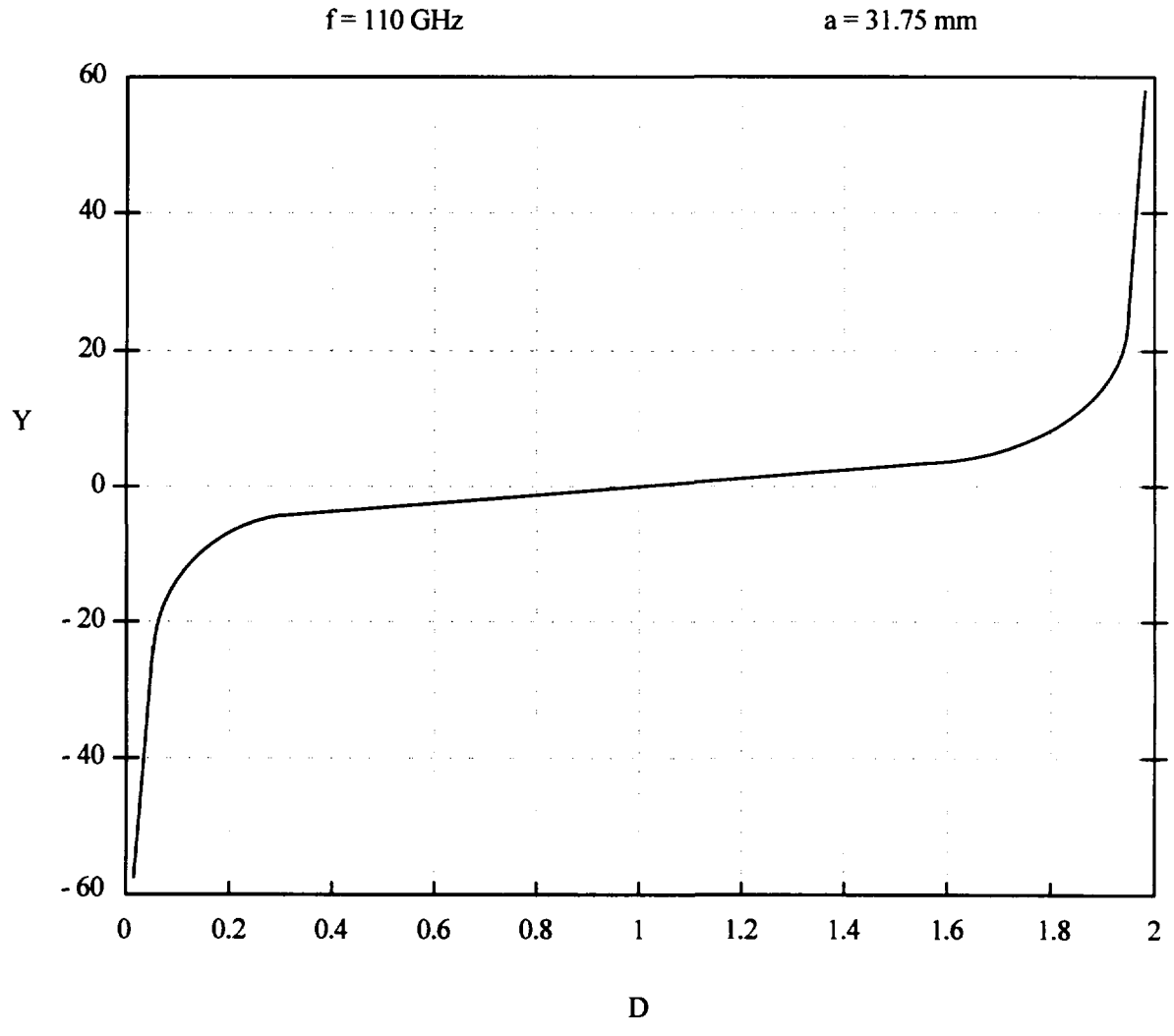

***Figure 5** : Variations of the wall function Y for w/h = 0.5*

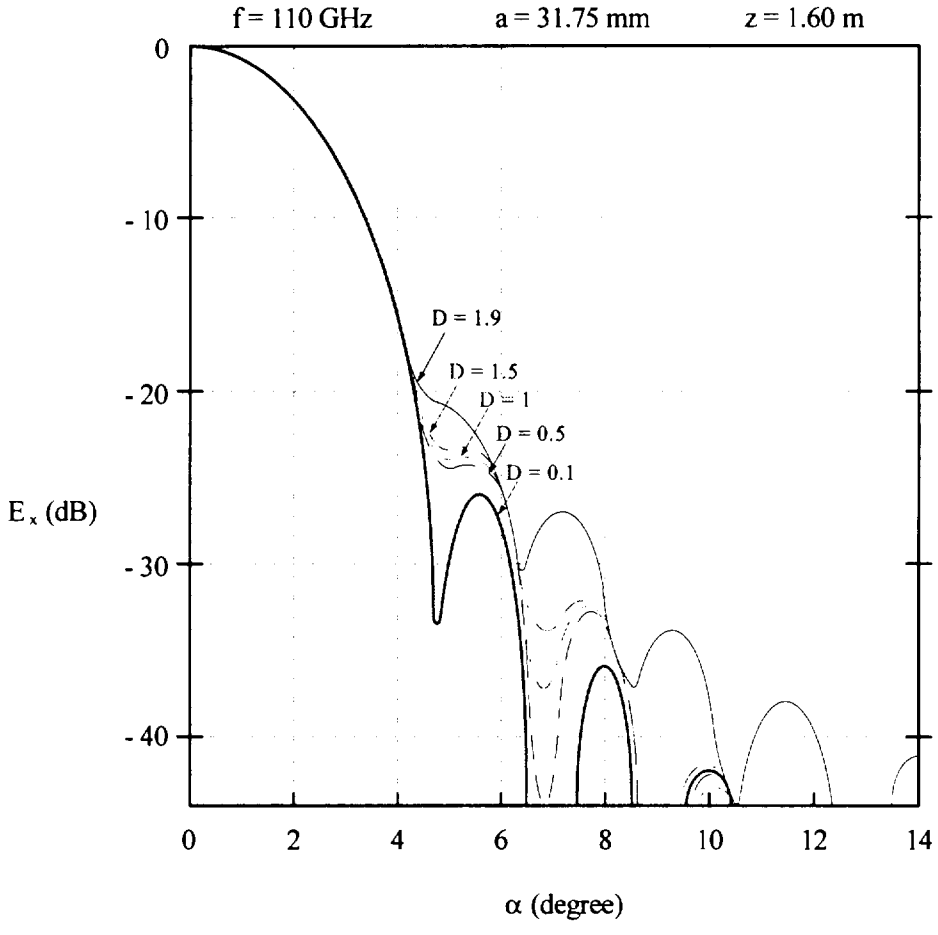

***Figure 6* : Radiation patterns of the HE_{11} mode for $\phi = 0$**

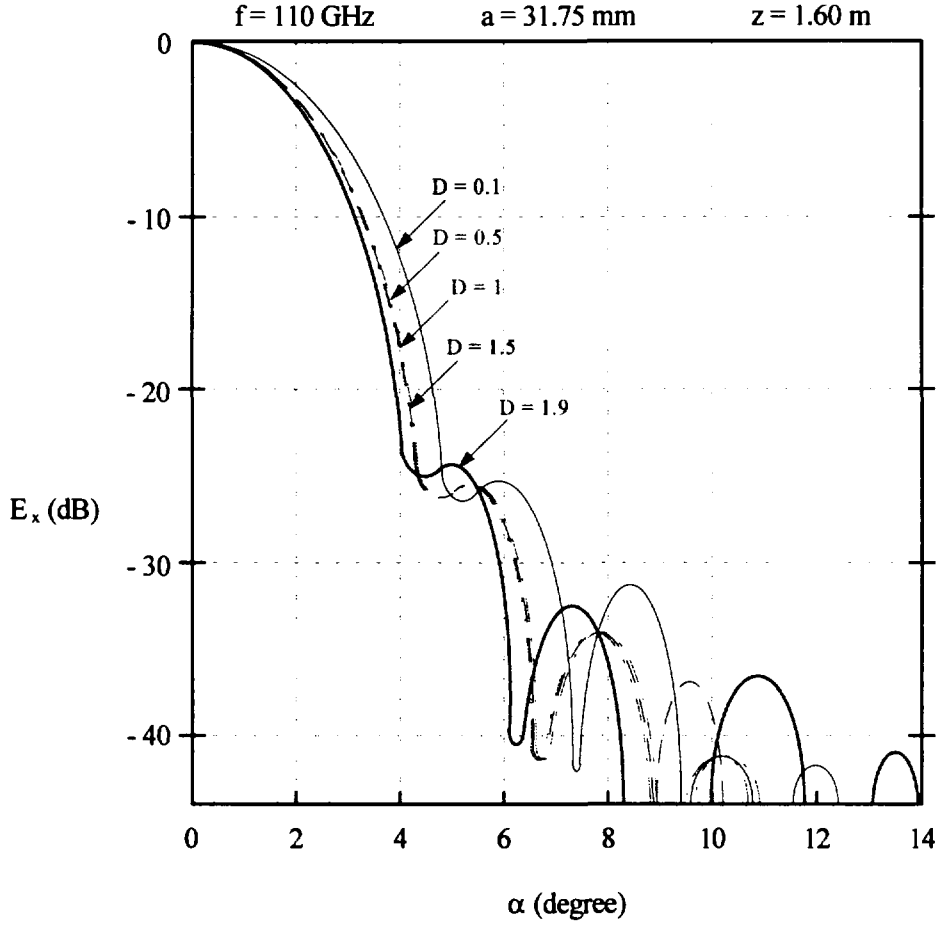

Figure 7 *: Radiation patterns of the* HE_{11} *mode for* $\phi = \pi/4$

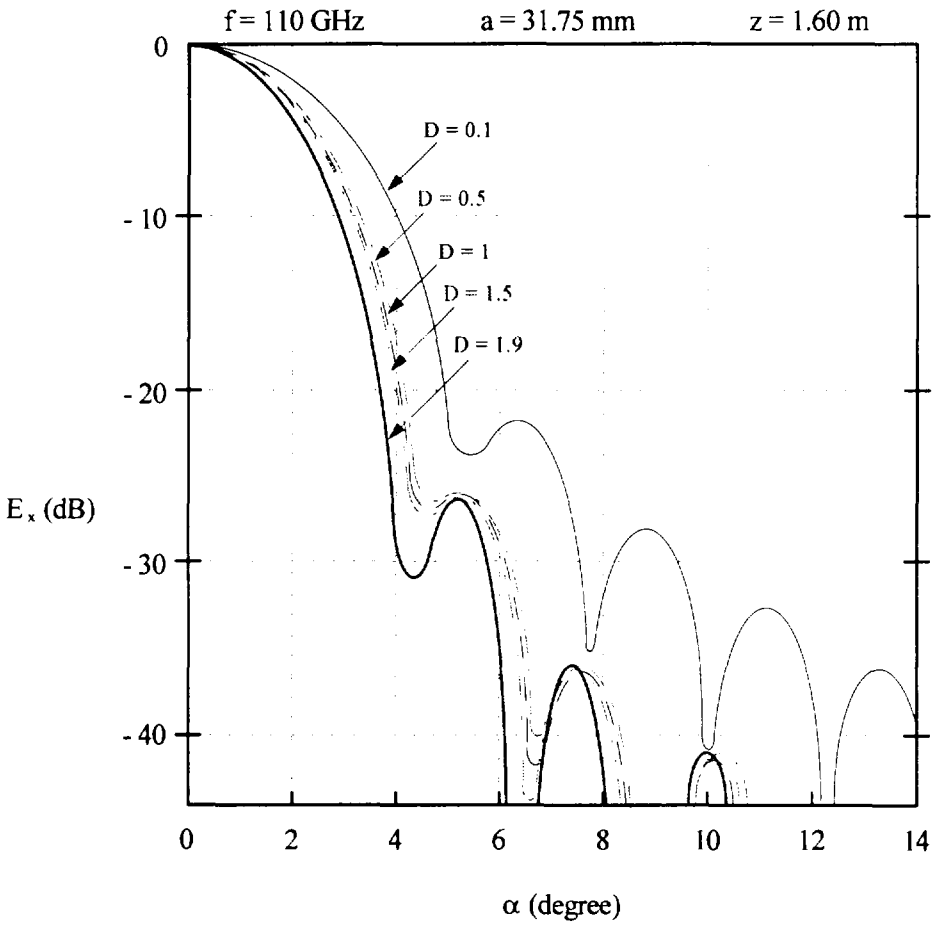

***Figure 8* : Radiation patterns of the HE_{11} mode for $\phi = \pi/2$**

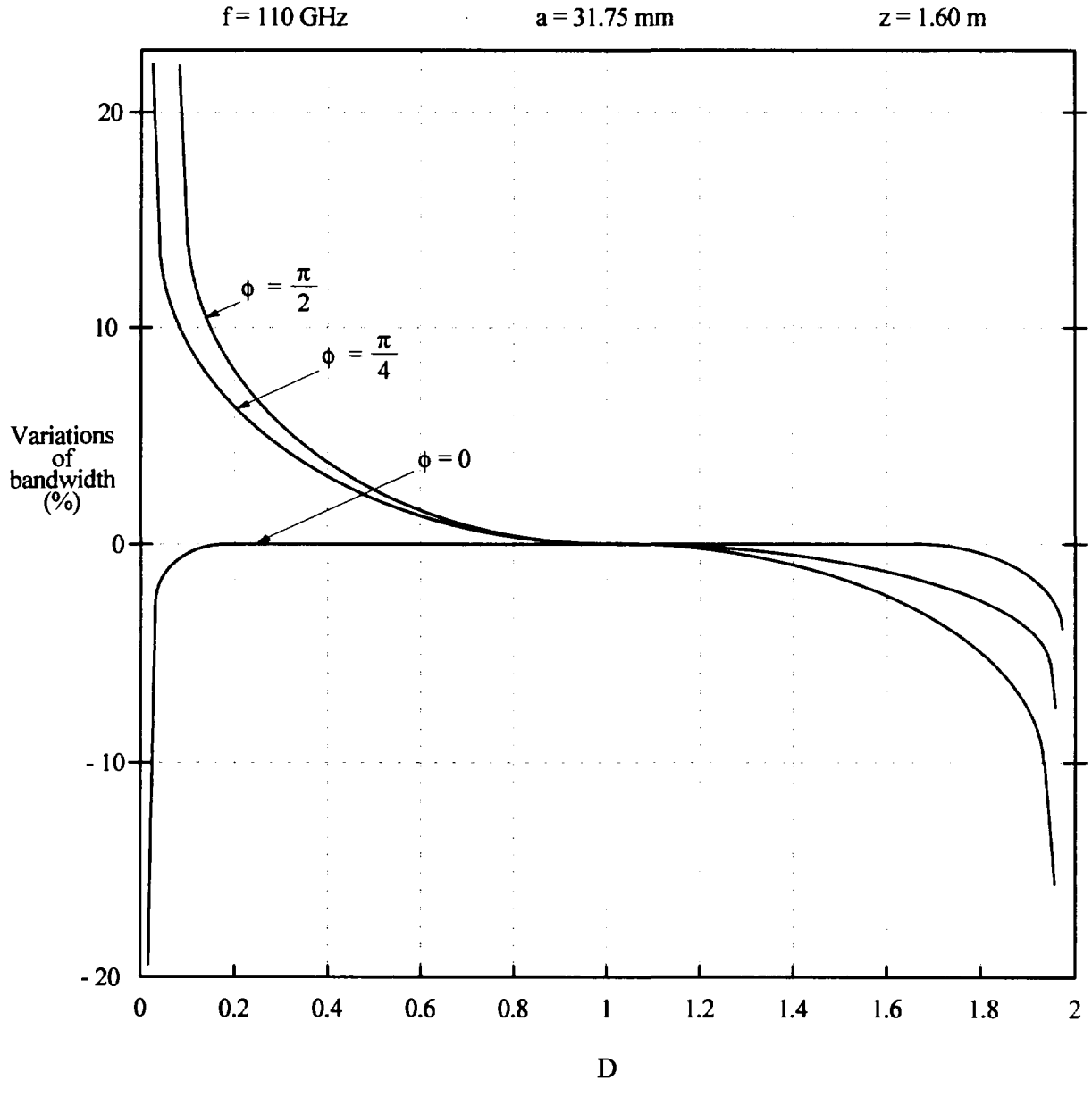

***Figure 9** : Variations of the 10 dB bandwidth of E_x referred to the case D = 1 and for w/h = 0.5*

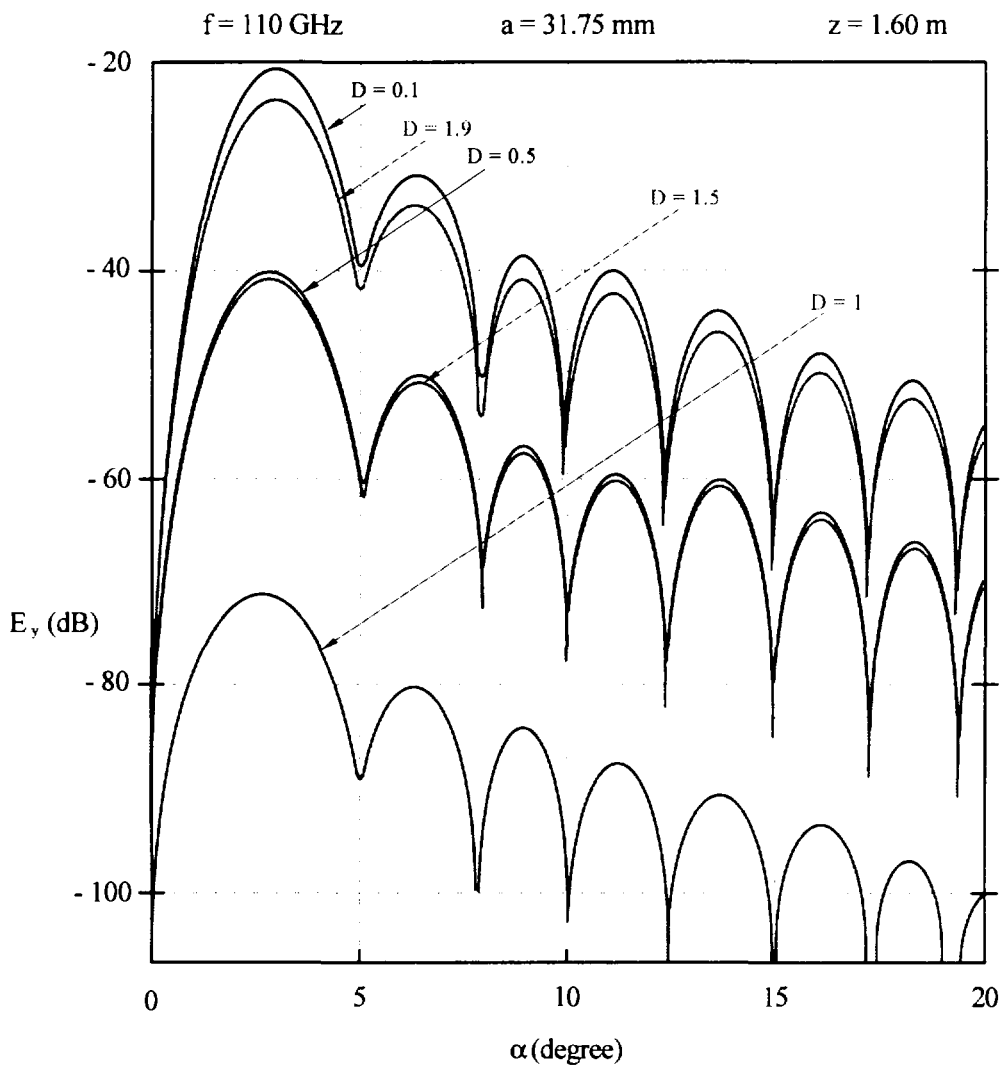

***Figure 10** : Cross-polarization of HE_{11} mode normalized to $E_x(0) = 1$ and for $\phi = \pi/4$*

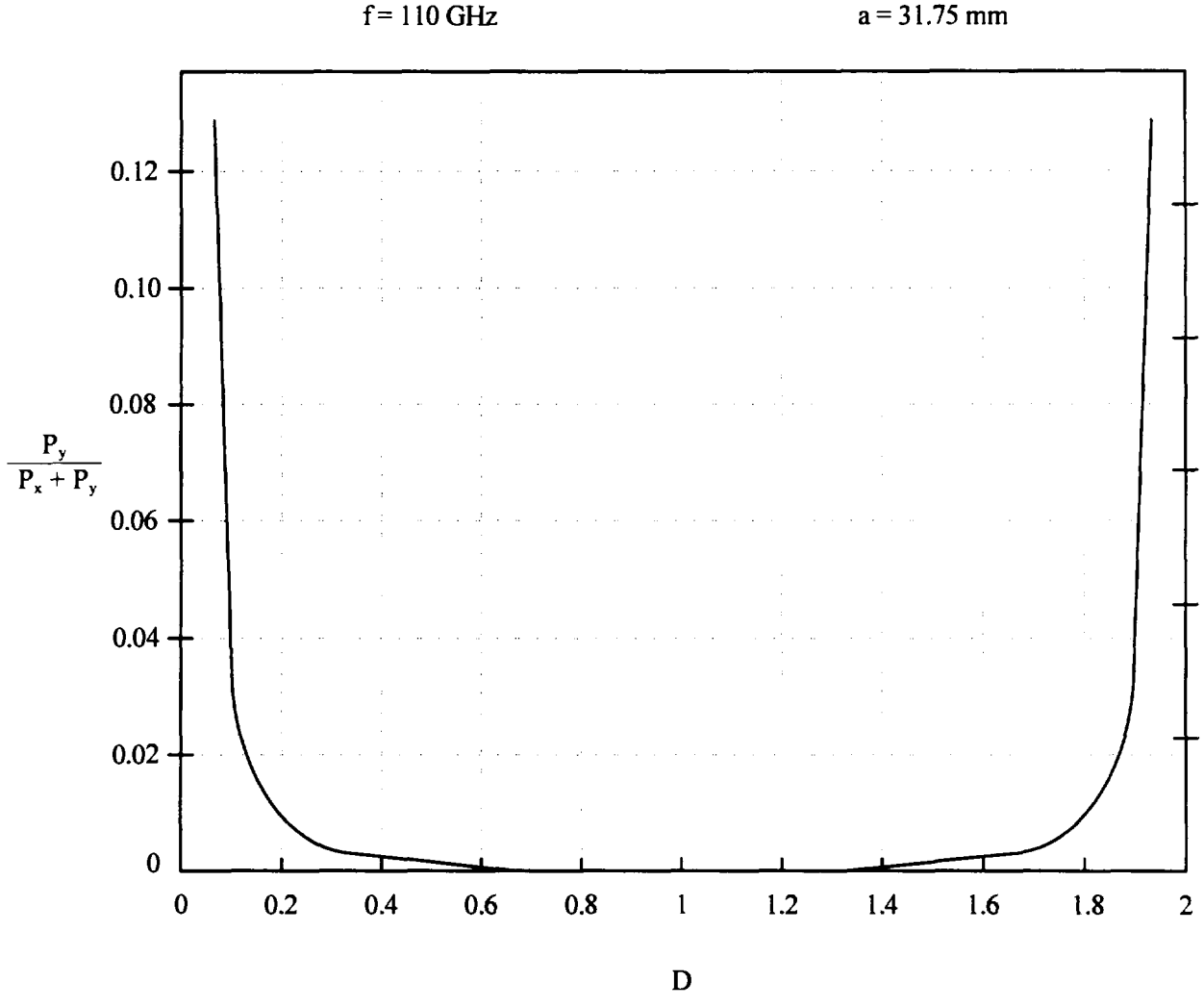

***Figure 11** : Variations of* $\frac{P_y}{P_y + P_x}$ *for w/h = 0.5*

f = 110 GHz a = 31.75 mm $\frac{w}{h} = 0.5$

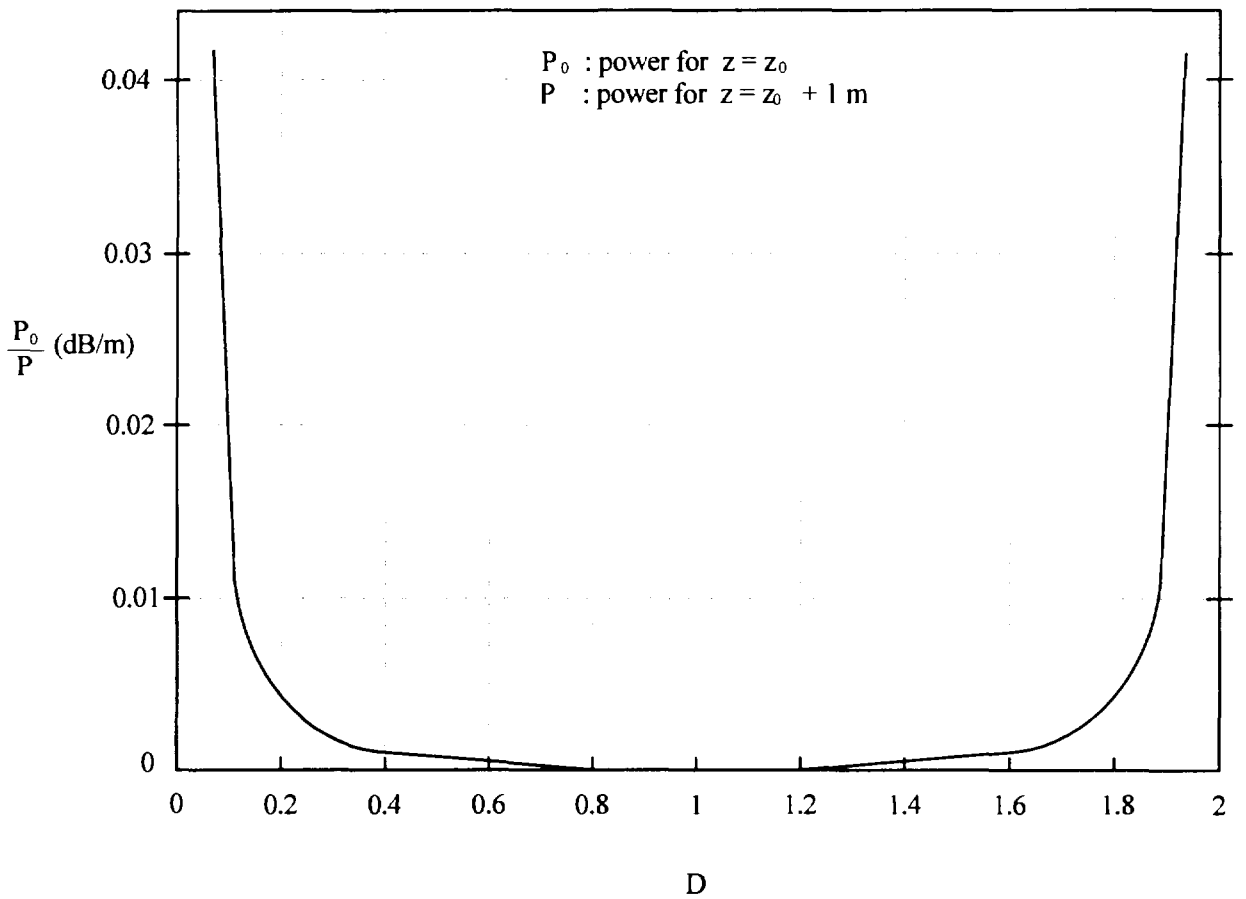

***Figure 12* : Attenuation of the HE_{11} mode**

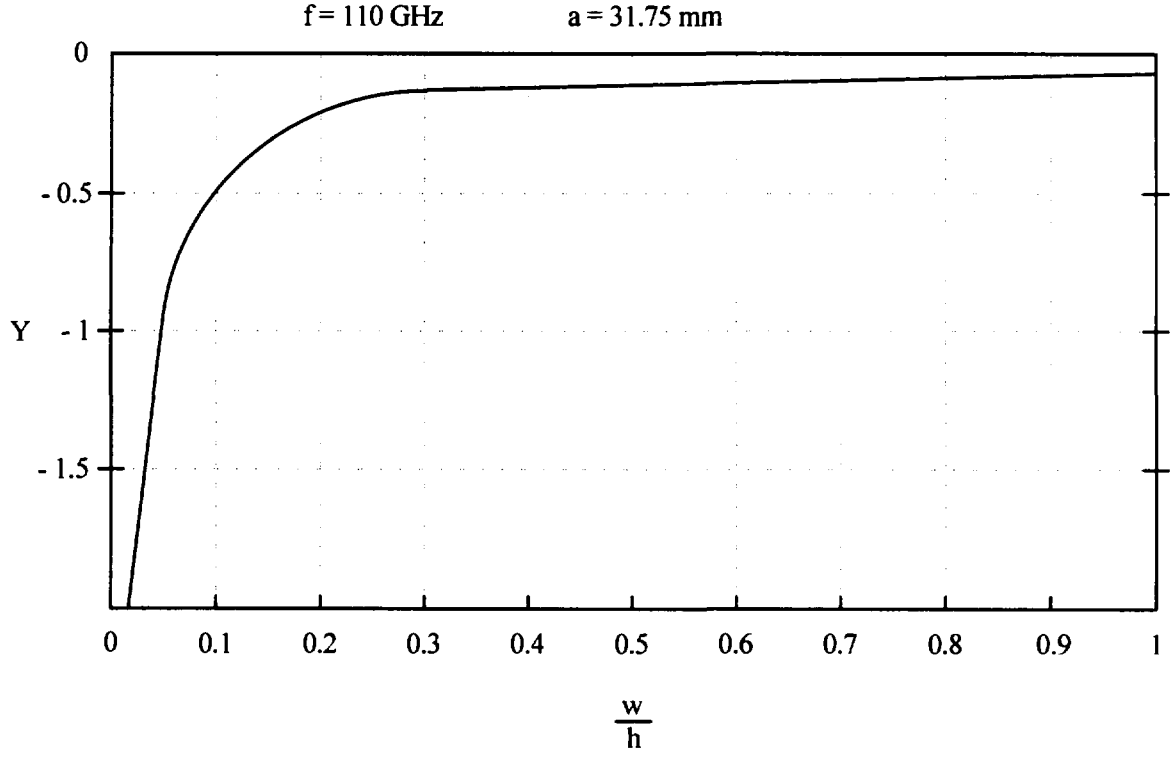

***Figure 13** : Variations of the wall function Y for D = 1*

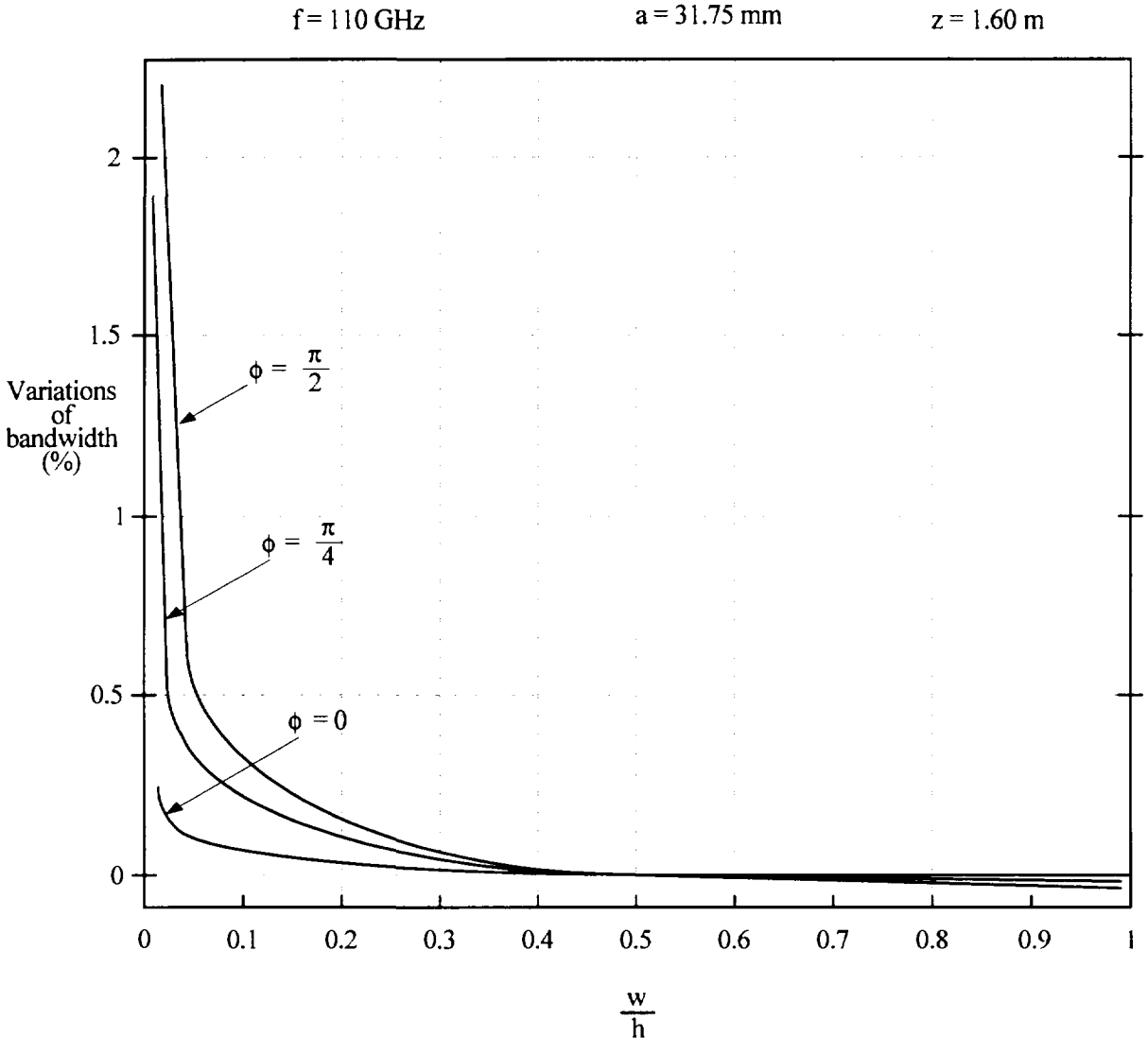

***Figure 14** : Variations of the 10 dB bandwidth of E_x referred to the case w/h = 0.5 and for D = 1*

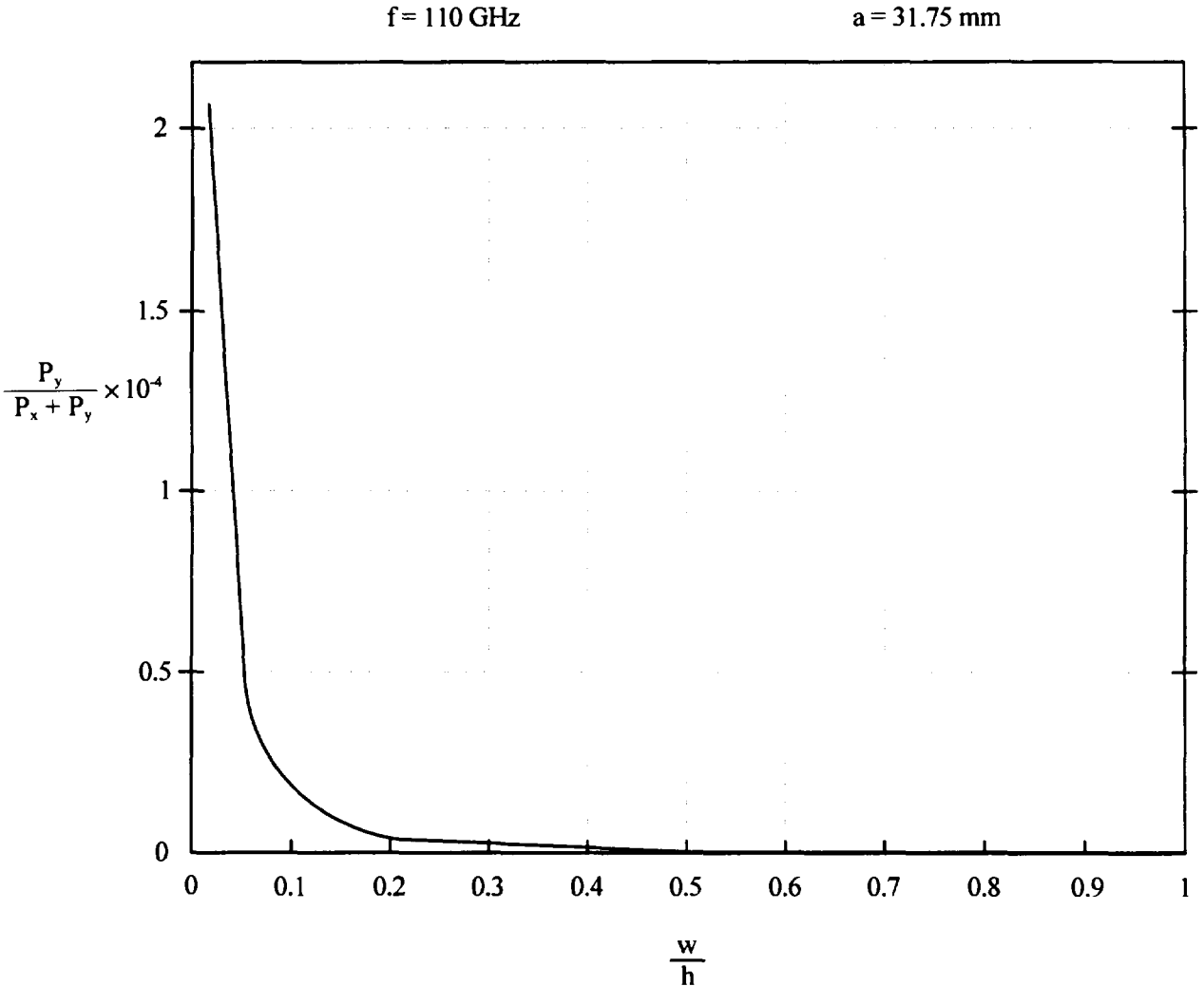

***Figure 15** : Variations of* $\frac{P_y}{P_y + P_x}$ *for D = 1*

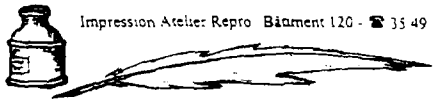
Impression Atelier Repro Bâtiment 120 - ☎ 35 49